




Cite this: *Nanoscale*, 2019, **11**, 8597

Substituent effects of AIE-active α -cyanostilbene-containing triphenylamine derivatives on electrofluorochromic behavior†

Sin-Yu Chen,^a Ya-Wen Chiu^a and Guey-Sheng Liou  ^{*a,b}

Four aggregation-induced emission (AIE)- and electro-active cyanostilbene-based triphenylamine-containing derivatives with different substituents were synthesized to investigate their effects on the photoluminescence properties and electrochromic (EC) and electrofluorochromic (EFC) behavior of gel-type electrochromic devices (ECDs). The optical and photoluminescence properties of the obtained materials were influenced by the substituents, and revealed AIE-active characteristics, exhibiting stronger fluorescence intensity in the aggregated state than in solution. Consequently, the EFC devices could be fabricated by combining these AIE- and electro-active materials with cathodic EC heptyl viologen HV into the gel-type electrolyte system to enhance the emission intensity, on/off contrast ratio, and response capability.

Received 28th March 2019,
Accepted 4th April 2019

DOI: 10.1039/c9nr02692d

rsc.li/nanoscale

Introduction

Organic materials with efficient emission in the solid state are necessary for optoelectronic devices. Such devices include organic light-emitting diodes, organic light-emitting field-effect transistors and organic fluorescent sensors.^{1–3} Therefore, innovations in novel luminescent materials emitting fluorescence in the solid state with high efficiency are a major objective for researchers, as is their modification and application. Nevertheless, most organic fluorophores are strongly emissive in solution but faintly emissive in the solid state on account of concentration quenching resulting from intermolecular interactions (*e.g.* energy transfer in the aggregated state and excimer formation). Recently, a phenomenon contrary to traditional aggregation-caused quenching (ACQ) has been discovered: a silole derivative was shown to emit weak fluorescence in solution but emitted light gradually as the amount of a poor solvent increased in the solution.⁴ This condition is called “aggregation-induced emission” (AIE), whereby molecules can be highly emissive in an aggregated

state (*e.g.* nanoparticle aggregates, thin films, powders and crystals) to facilitate more optoelectronic applications.⁵

Bifunctional fluorescent molecular switches were first fabricated by Lehn *et al.*⁶ Subsequently, electrofluorochromic (EFC) devices were prepared with different electroactive fluorophores: small organic molecules, inorganic materials, and high-performance polymers.^{7–9} Electrofluorochromism is a phenomenon usually associated with electrochromism (EC) of electroactive fluorophores during redox reactions. Kim and Audebert were the first to prepare an EFC device by blending a tetrazine derivative with a polymer electrolyte.^{10,11} Our research team has also fabricated flexible devices with excellent switching ability from a fluorescent neutral state to a non-fluorescent monocation radical state with high contrast ratios and low applied potentials using electroactive polymer films with an aggregation-enhanced emission (AEE) effect.^{12–14}

Triphenylamine (TPA) has several advantageous features, such as good solubility, photoluminescence (PL) and EC behavior, but it shows an ACQ effect, which is a drawback for practical applications. According to Tang and colleagues, ACQ-luminogens (gens) would change to AIE-gens by incorporation of AIE fluorophores into ACQ structures.¹⁵ This type of approach is facile and effective for obtaining AIE-gens.^{16–18} Moreover, a cyanostilbene moiety has been utilized frequently as a functional unit in the design of advanced optical materials because of its simple structure and high polarizability.¹⁹ The resulting derivatives display AIE features because the cyano group can provide not only a steric effect to prevent close π - π stacking but also intermolecular hydrogen bonding to rigidify molecules.

^aInstitute of Polymer Science and Engineering, National Taiwan University, 1 Roosevelt Road, 4th Sec., Taipei 10617, Taiwan. E-mail: gsliau@ntu.edu.tw; Tel: +886-2-33665070

^bAdvanced Research Center for Green Materials Science and Technology, National Taiwan University, Taipei 10617, Taiwan

† Electronic supplementary information (ESI) available. CCDC 1894255–1894257. For ESI and crystallographic data in CIF or other electronic format see DOI: 10.1039/c9nr02692d

Hence, electroactive TPA with an ACQ effect was designed to be combined with AIE-active cyanostilbene to obtain a series of AIE molecules with highly emissive characteristics in the solid state. In addition, a gel-type electrolyte system could be applied to limit the intramolecular motion of AIE molecules to obtain EFC devices with strong fluorescence. Furthermore, the cathodic EC material of heptyl viologen (HV) could be introduced to act as the “counterion reservoir” for shortening the EC switching time and enhancing the contrast ratio of EFC devices.

Experimental section

Materials

Commercially available diphenylamine (Alfa), 4-bromobenzaldehyde (AK Scientific), phenylacetonitrile (ACROS), 4-bromophenylacetonitrile (Alfa), *p*-anisidine (ACROS), 4-bromoanisole (Alfa) and other reagents were used as received. The cathodic EC material heptyl viologen tetrafluoroborate HV(BF₄)₂ was prepared.²⁰ Briefly, 4,4'-dipyridyl (3.12 g, 20 mmol) and 1-bromoheptane (31.4 mL, 200 mmol) were added to 30 mL of acetonitrile and refluxed for 6 h. The precipitate was filtered off after cooling down to room temperature. It was washed with organic solvents such as hot chloroform, acetone and hexane, and then dried in a vacuum to obtain a 96% yield of yellow powder HVBr₂ (9.85 g). Afterwards, the solution of HVBr₂ (5.00 g) in deionized water (50.0 mL) was added dropwise to a saturated solution of NaBF₄ (50.0 mL). After 30 min, a white solid HV(BF₄)₂ was obtained after filtration, then purified by recrystallization from ethanol.

Synthesis of TPA-based electroactive materials

Aldehyde derivatives (TPA-CHO and diOMe-TPA-CHO) and phenylacetonitrile (or 4-bromophenylacetonitrile) were used to synthesize the AIE-active α -cyanostilbene-containing TPA luminogens (TPA-CN, diOMe-TPA-CN, TPA-CNBr and diOMe-TPA-CNBr), respectively, by the Knoevenagel condensation (Scheme S1†). Taking TPA-CN as an example, a solution of potassium hydroxide (KOH, 0.17 g, 3.0 mmol) in 10 mL of ethanol was added dropwise to a mixture of TPA-CHO (0.55 g, 2.0 mmol) and phenylacetonitrile (0.35 g, 3.0 mmol) in ethanol (10 mL) at room temperature. After stirring for 24 h, a bright-yellow solid was obtained during the reaction. The resulting crude product was dried to afford a yellow solid (0.65 g, 87%) and purified by recrystallization.

Fabrication of a gel-type EFC device

The procedure to prepare a gel-type EFC device is depicted in Fig. S1.† Two ITO ($\sim 5 \Omega$ per square) glasses were confined to a 120 μm gap by curing a thermoset adhesive with an active area of $2 \times 2 \text{ cm}^2$ at 120 °C for 6 h. A small opening was retained for injecting materials into the device through a vacuum-encapsulating method. The gel-type device contained 0.75 μM (0.015 M) of EFC materials and a HV, a copolymer of methyl methacrylate (MMA) and 2-hydroxyethyl methacrylate (HEMA)

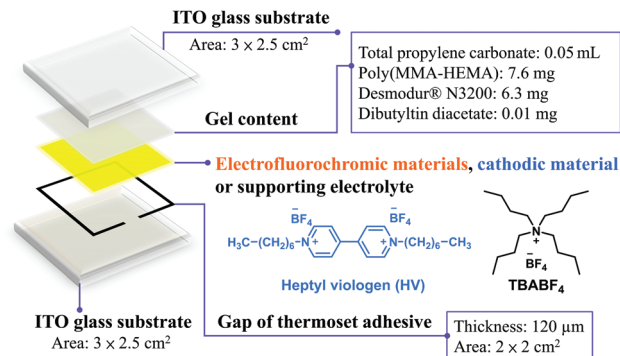


Fig. 1 Composition of EFC devices.

(poly(MMA-HEMA), 7.6 mg), an aliphatic polyisocyanate (Desmodur® N3200, 6.3 mg) and a catalyst (dibutyltin diacetate, 0.01 mg) dissolved in 0.05 mL propylene carbonate (Fig. 1). After injection, the opening was sealed *via* a UV-curing adhesive, and then was cured at 75 °C for 2 h to obtain the crosslinked gel-type EFC device.

Results and discussion

Monomer synthesis and characterization

The synthetic procedure of TPA-based aldehyde derivatives is depicted in Scheme S1.† 4-Aldehyde-triphenylamine (TPA-CHO) and 4-aldehyde-4',4''-dimethoxytriphenylamine (diOMe-TPA-CHO) were synthesized according to procedures described previously.^{21,22} Then, phenylacetonitriles were reacted with aldehyde derivatives to afford 2-(phenyl)-3-[4-(*N,N*-diphenylamino)phenyl]acrylonitrile (TPA-CN), 2-(phenyl)-3-[4-bis(4-methoxyphenylamino)phenyl]acrylonitrile (diOMe-TPA-CN), 2-(4-bromophenyl)-3-[4-(*N,N*-diphenylamino)phenyl]acrylonitrile (TPA-CNBr) and 2-(4-bromophenyl)-3-[4-bis(4-methoxyphenylamino)phenyl]acrylonitrile (diOMe-TPA-CNBr) with yields >75%.^{21–24} All compounds were purified by recrystallization and characterized clearly by nuclear magnetic resonance (NMR) spectroscopy. The structure of the new compound, diOMe-TPA-CN, was identified further by 2D ¹H–¹H correlated spectroscopy (COSY) and 2D ¹H–¹³C heteronuclear single quantum coherence (HSQC) NMR spectroscopy (Fig. S2–5†) and elemental analyses.

Optical properties

The optical properties of the α -cyanostilbene-containing TPA derivatives were investigated by UV-vis spectrophotometry and PL spectroscopy. The UV-Vis absorption and PL emission spectra of all of the chromogens in DMSO solution and solid state are depicted in Fig. 2. Compounds with bromide and dimethoxy auxochromes exhibited a bathochromic effect not only on the maximum absorption peaks (λ_{abs}) but also maximum emission peaks (λ_{em}) in DMSO solution and in the solid state. Incorporating bromide and dimethoxy groups into the structure of the materials would endow stronger donor–

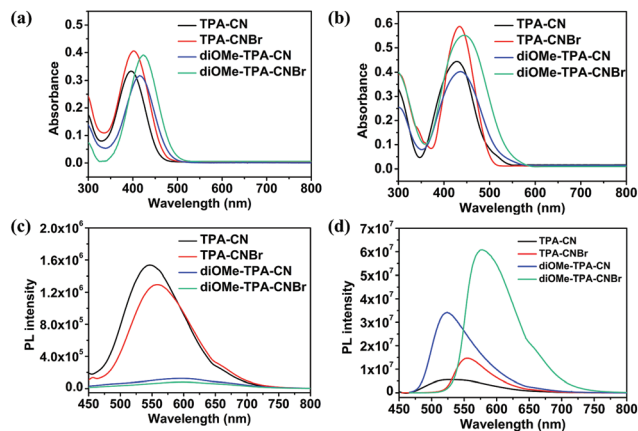


Fig. 2 Absorption spectra of TPA-CN, TPA-CNBr, diOMe-TPA-CN and diOMe-TPA-CNBr in (a) DMSO solution (10 μM) and (b) solid state. PL spectra of TPA-CN, TPA-CNBr, diOMe-TPA-CN and diOMe-TPA-CNBr in (c) DMSO solution (10 μM) and (d) solid state.

acceptor abilities, thereby resulting in enhanced red-shift behavior. Photographs taken under UV illumination also showed consistency with the results mentioned above, and all of the optical characteristics are listed in Table 1.

Photoluminescence properties

Photoluminescence properties were evaluated at 10 μM of the prepared compounds in various water/DMSO fractions ($f_w = 0\text{--}99\%$). The molecular dispersion of nanoscale aggregates appeared upon increasing of the water content of the water/DMSO mixture. Consequently, intramolecular motions could be restricted effectively because of aggregation, resulting in greatly intensified light emission.

These electro-active cyanostilbene-based TPA derivatives all displayed AIE features with various emissive behavior in solution and aggregated states. Fig. 3 illustrates the AIE character-

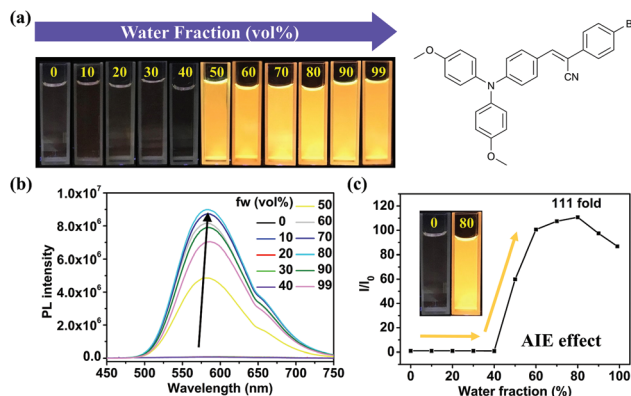
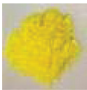
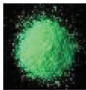

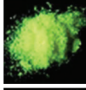

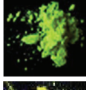




Fig. 3 (a) Images of diOMe-TPA-CNBr taken under UV light at different water/DMSO fractions. (b) PL spectra of diOMe-TPA-CNBr in DMSO and water/DMSO mixtures with different water fractions (f_w). (c) Plot of relative emission intensity (I/I_0) versus the composition of aqueous mixtures of diOMe-TPA-CNBr. I_0 = Emission intensity in pure DMSO 10 μM solution, λ_{ex} : 423 nm.

istics of diOMe-TPA-CNBr. The emission peak of diOMe-TPA-CNBr appears at 599 nm with 0.10% PL quantum yield (Φ_F) in pure DMSO solution, estimated using quinine sulfate as a standard ($\Phi_F = 0.546$ dissolved in 1 N H_2SO_4 in 10 μM concentration), indicating weak emitting ability in the dilute solution state. When a poor solvent (water) was increasingly added to the solution before f_w achieved 50%, the PL intensity of diOMe-TPA-CNBr was almost consistent with the condition of the pure solution, and the other materials also exhibited similar PL behaviour, as shown in Fig. S6–S8.† Among the four compounds, the α_{AIE} values ($\alpha_{\text{AIE}} = \Phi_F(\text{solid})/\Phi_F(\text{solution})$) of diOMe-TPA-CNBr and diOMe-TPA-CN could be massively enhanced (diOMe-TPA-CNBr = 710, diOMe-TPA-CN = 220) when compared to the ones without dimethoxy groups (TPA-CNBr = 19.8, TPA-CN = 9.3). Furthermore, by introducing

Table 1 Photoluminescence properties of TPA-CN, TPA-CNBr, diOMe-TPA-CN and diOMe-TPA-CNBr and their images taken under UV illumination (365 nm)

	λ_{abs}^a (solution)	λ_{em}^a (solution)	λ_{abs} (solid)	λ_{em} (solid)	λ_{onset} (solid)	Φ_F^b (%) (solution)	Φ_F^c (%) (solid)	α_{AIE}^d	Under room light	Under UV light (365 nm)
TPA-CN	396	546	429	527	496	1.57	14.6	9.3		
TPA-CNBr	402	558	434	554	503	1.10	21.8	19.8		
diOMe-TPA-CN	415	596	438	533	529	0.20	44.3	220.2		
diOMe-TPA-CNBr	423	599	446	577	548	0.10	73.6	710.5		

^a Observed from absorption and emission spectra in dilute DMSO solution (10^{-5} M). ^b Fluorescence quantum yield determined by using quinine sulfate ($\Phi_F = 54.6\%$ in 0.1 N sulfuric acid) as a standard. ^c Fluorescence quantum yield determined by a calibrated integrating sphere. ^d $\alpha_{\text{AIE}} = \Phi_F(\text{solid})/\Phi_F(\text{solution})$.

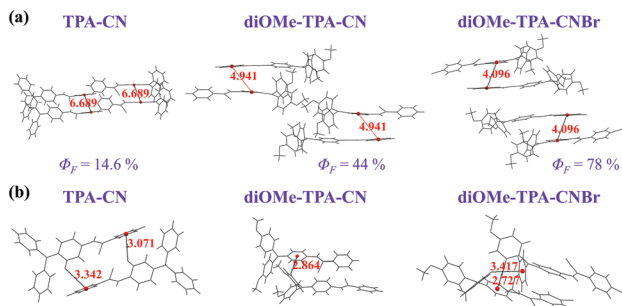


Fig. 4 Single-crystal packing structures of prepared compounds. (a) π - π interactions and (b) C-H... π interactions of TPA-CN, diOMe-TPA-CN and diOMe-TPA-CNBr.

dimethoxy groups into molecular structures, the stronger donor-acceptor effect brings about absorption and emission peaks to a longer wavelength, which is an additional benefit for tuning the color of the emitted light.

To understand further the photophysical properties of these luminogens in the solid state, their molecular conformations and packing models in single crystals were obtained (Fig. 4 and Tables S1-3[†]). A π - π interaction could occur because the face-to-face distance between two molecular planes was <3.5 Å. That is, fluorescence quenching could occur if the face-to-face distance of two planes was <3.5 Å (π - π stacking). Moreover, a C-H... π interaction is defined as an interaction which could appear if the distance between a face of an aromatic ring and another hydrogen atom within two molecular chains is <3.5 Å. Meanwhile, more C-H... π interactions can rigidify molecular chains to suppress intramolecular motions and closer molecular packing, resulting in higher PL quantum yields in the solid state.

According to the results depicted in Fig. 4, the shortest interplanar distance between α -cyanostilbene units in TPA-CN, diOMe-TPA-CN and diOMe-TPA-CNBr was 6.689, 4.941 and 4.096 Å, respectively, indicating that all structures beyond 3.5 Å had π - π interactions. Hence, these three structures exhibited AIE properties. Moreover, the shortest distance of C-H... π interactions was found in the structure of diOMe-TPA-CNBr, which elicited the highest PL quantum yield in the solid state and an AIE characteristic (α_{AIE}) value.

Electrochemical stability of materials

To fabricate electrochemically stable EFC devices, the electrochemical stability of these four electroactive materials was confirmed first by repetitive cyclic voltammetry (CV). TPA derivatives without any protecting groups at the *para*-position of the phenyl rings are not stable under redox reactions.^{25,26} Thus, the molecular structures without dimethoxy protecting groups (TPA-CN and TPA-CNBr) exhibited different CV behavior compared with the first cycle with respect to lower electric current intensity and lower E_{onset} in CV curves (Fig. 5a and b). This lower E_{onset} could be ascribed to the extent of formation of a dimer structure of benzidine (which arose from the dimerization of TPA⁺ during oxidation), with higher ox-

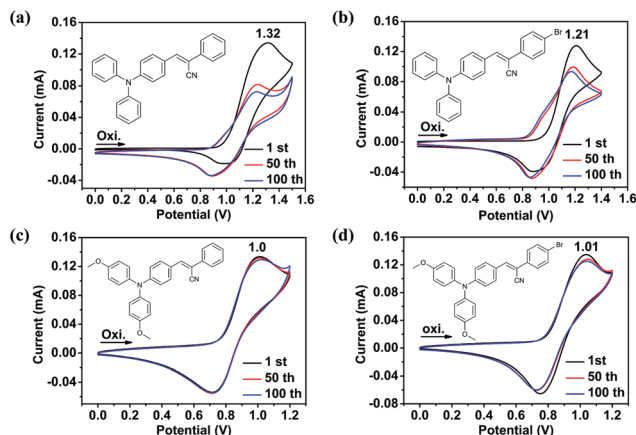


Fig. 5 Repetitive cyclic voltammograms (scan rate: 50 mV s^{-1}) of (a) TPA-CN, (b) TPA-CNBr, (c) diOMe-TPA-CN and (d) diOMe-TPA-CNBr by OTTE for 50 cycles and 100 cycles at a concentration of $10 \mu\text{M}$ in $0.1 \text{ M TBABF}_4/\text{PC}$ solution.

idation stability and lower oxidation potential.²⁷ diOMe-TPA-CN and diOMe-TPA-CNBr with dimethoxy groups exhibited lower oxidation potentials and highly electrochemical stability (Fig. 5c and d) due to the electron-donating capability of dimethoxy groups.²⁸ Therefore, in the subsequent preparation of an EFC device, diOMe-TPA-CN and diOMe-TPA-CNBr were fabricated and the EFC behavior of the obtained devices studied.

Electrochemical properties of gel-type EFC devices

CV was used to measure the electrochemical properties of gel-type EFC devices derived from diOMe-TPA-CN/HV and diOMe-TPA-CNBr/HV. The cation of HV, HV²⁺, could accept electrons from TPA units and become HV⁺ when oxidation occurred. Conversely, HV⁺ served as an electron donor to TPA⁺ during reduction. Therefore, HV introduced into devices served as an effective counter-ion reservoir for decreasing the applied potential, rapidly balancing charges during EC switching, and even enhancing the EC performance. Consequently, oxidation potentials for these two systems could be fixed at 1.91 V for diOMe-TPA-CN/HV and 1.90 V for diOMe-TPA-CNBr/HV (Fig. 6).

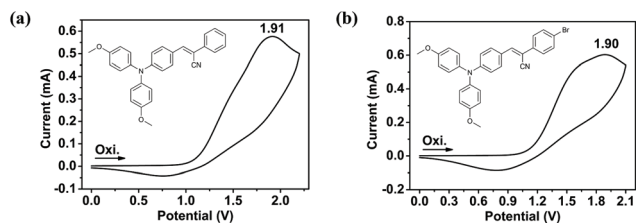


Fig. 6 Cyclic voltammograms (scan rate: 50 mV s^{-1}) of EFC devices based on (a) $0.75 \mu\text{M}$ diOMe-TPA-CN, (b) $0.75 \mu\text{M}$ diOMe-TPA-CNBr, both with $0.75 \mu\text{M}$ HV.

Spectroelectrochemical properties of gel-type EFC devices

The EC behavior of these EFC devices based on **diOMe-TPA-CN/HV** and **diOMe-TPA-CNBr/HV** was investigated, and the resulting spectroelectrochemical spectra are displayed in Fig. S9.† Characteristic absorption peaks were observed at 517, 606 and 760 nm for **diOMe-TPA-CN/HV**, and at 520, 606 and 760 nm for **diOMe-TPA-CNBr/HV**, respectively. Color changes could be defined by CIELAB coordinates where **diOMe-TPA-CN/HV** changed from (91.22, -18.22, 78.63) at 0.0 V in the neutral form to (67.62, -18.37, 53.21) in the oxidation state at 1.8 V, and **diOMe-TPA-CNBr/HV** changed from (91.07, -15.47, 95.73) at 0.0 V to (67.75, -11.38, 69.13) at 1.8 V.

EFC properties of gel-type devices

Based on our previous research, the supporting electrolyte could be replaced by HV.^{29,30} Accordingly, the devices were prepared without a supporting electrolyte. AIE-active **diOMe-TPA-CN** and **diOMe-TPA-CNBr** had high PL quantum yields of 44.3% and 73.6% in the solid state, respectively. Therefore, gel-type EFC devices based on **diOMe-TPA-CN** and **diOMe-TPA-CNBr** were fabricated to inhibit and restrict the intramolecular motion of AIE molecules by producing a fraction of crosslinking moieties to obtain stronger PL intensity. In addition, because of the electroactive TPA units within these molecular structures, the EFC devices showed obvious changes in optical absorption during oxidation. The specific absorption peaks could also quench the light emission of fluorophores and then bring about EFC behavior with higher PL contrast ratios ($I_{\text{off}}/I_{\text{on}}$) between the neutral fluorescent state and oxidized non-fluorescent state. Introducing the cathodic material HV into the device shortened the response time (Fig. S11†) and lowered the applied potential but also added an extra absorption peak at 606 nm, which was expected to absorb the emission from fluorophores because the emission peaks of the EFC materials were close to the characteristic peak of HV.

As shown in Fig. 7a and 8a, the PL intensity of the gel-type EFC devices based on **diOMe-TPA-CN/HV** and **diOMe-TPA-CNBr/HV** systems decayed with increasing applied oxidation potentials. Upon application of voltages from 0 to 1.8 V, the PL intensity of the gel-type device with **diOMe-TPA-CN/HV** was reduced, and the PL contrast ratio $I_{\text{off}}/I_{\text{on}}$ was ~ 6.75 (Fig. 7b). Similarly, the PL intensity of the gel-type device with **diOMe-TPA-CNBr/HV** decreased at higher voltages, and achieved a PL contrast ratio of 6.76 upon applying voltages between 0 to 1.8 V (Fig. 8b). The fluorescence switching responses for these two systems are illustrated in Fig. 7c, d and 8c, d. They demonstrate that the **diOMe-TPA-CNBr/HV** system had a shorter response time than the **diOMe-TPA-CN/HV** system under their light-emission wavelengths. Furthermore, the long-term stability and reversibility of the resulting EFC devices were investigated by measuring the PL intensity as a function of the switching cycles shown in Fig. 9. The recovery of EFC devices of **diOMe-TPA-CN/HV** and **diOMe-TPA-CNBr/HV** was 96% and 98% after 100 and 150 cycles, respectively. The higher EFC reversibility for **diOMe-TPA-CNBr/HV**

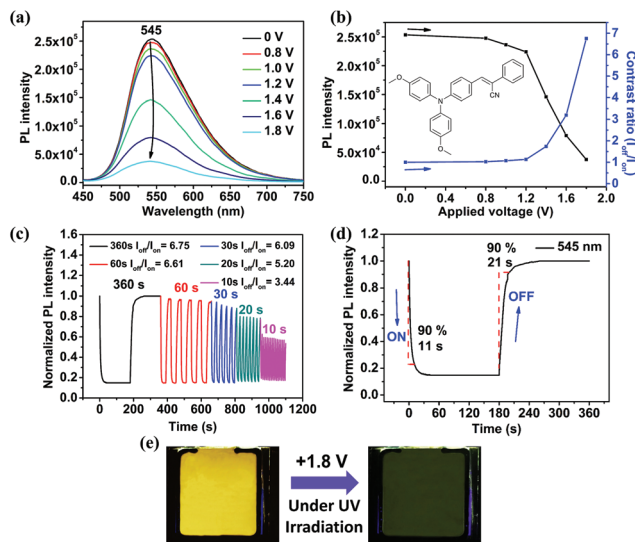


Fig. 7 (a) PL spectra as applying voltage between 0 and 1.8 V, (b) applied voltage vs. PL intensity and contrast diagram, (c) fluorescence switching response at different step cycle times of 360, 60, 30, 20, and 10 s, (d) estimation of fluorescence switching time of 0.75 $\mu\text{mole}/0.75 \mu\text{mole}$ **diOMe-TPA-CN/HV** between 1.8 (on) and -0.1 V (off) monitored at 545 nm ($\lambda_{\text{ex}} = 408$ nm), and (e) EFC behavior of gel-type device of 0.75 $\mu\text{mole}/0.75 \mu\text{mole}$ **diOMe-TPA-CN/HV**.

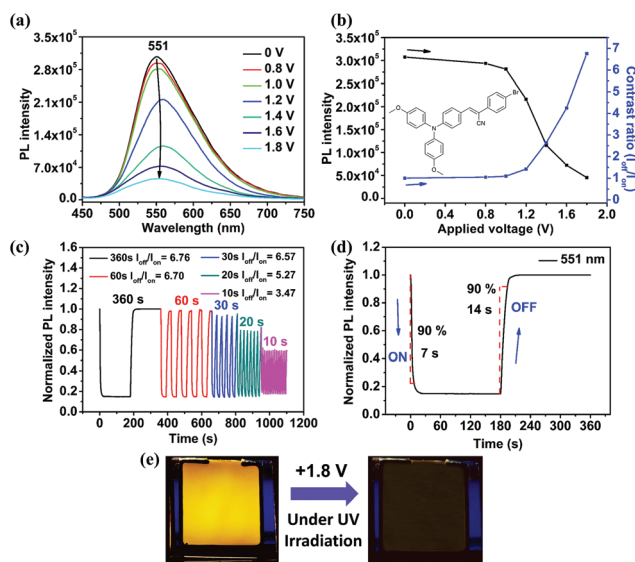


Fig. 8 (a) PL spectra at an applied voltage between 0 V and 1.8 V. (b) Applied voltage vs. PL intensity and contrast diagram. (c) Fluorescence switching response at different step cycle times of 360, 60, 30, 20, and 10 s. (d) Estimation of fluorescence switching time of 0.75 $\mu\text{M}/0.75 \mu\text{M}$ **diOMe-TPA-CNBr/HV** between 1.8 (on) and -0.1 V (off) monitored at 551 nm ($\lambda_{\text{ex}} = 413$ nm). (e) EFC behavior of a gel-type device of 0.75 $\mu\text{M}/0.75 \mu\text{M}$ **diOMe-TPA-CNBr/HV**.

HV could be attributed to the shorter EC response time and emission peak at 551 nm, which is closer to the 606 nm characteristic absorption peak from HV, resulting in lower decay when compared with that of **diOMe-TPA-CN**.

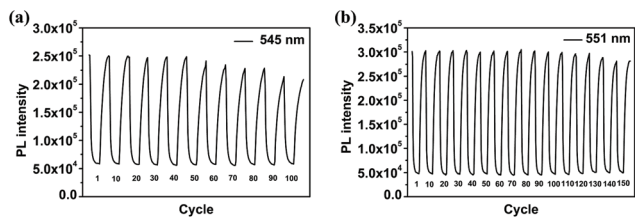


Fig. 9 Long-term stability and switching reversibility of EFC devices derived from (a) diOMe-TPA-CN/HV and (b) diOMe-TPA-CNBr/HV with a cycle time of 30 s.

Concentration effect of HV on the EFC behavior

To increase the PL contrast ratio of EFC devices, modulating the concentration is a feasible method. The diOMe-TPA-CN/HV system, with its high solubility (Table S4[†]), was chosen to demonstrate the concentration effect on EFC behavior. Two concentration ratios of the systems, 0.75/1.5 μM diOMe-TPA-CN/HV and 1.5/1.5 μM diOMe-TPA-CN/HV, were investigated, and their corresponding spectroelectrochemical behavior is depicted in Fig. S10.[†] The absorbance of all of the peaks for these two systems increased obviously compared with that of the original 0.75/0.75 μM diOMe-TPA-CN/HV system. In the system of 1.5 μM diOMe-TPA-CN and 1.5 μM HV (Fig. S10b[†]), the absorbances of all of the characteristic peaks were higher than those of 0.75/1.5 μM diOMe-TPA-CN/HV (Fig. S10a[†]) because one diOMe-TPA-CN molecule can match one HV molecule, resulting in a more dense color change. Consequently, the EFC behavior of these two diOMe-TPA-CN/HV concentrations could be improved owing to the higher absorbance of all characteristic peaks, particularly those at 517 and 606 nm.

The resulting EFC behavior with a modulated diOMe-TPA-CN/HV concentration was studied. The PL intensity of the gel-type EFC device in the 0.75/1.5 μM diOMe-TPA-CN/HV system (Fig. 10) revealed a PL $I_{\text{off}}/I_{\text{on}}$ contrast ratio of 8.15, which was higher than that of the original system (6.75) (Fig. 7b). Moreover, the PL contrast ratio of the 1.5 $\mu\text{M}/1.5 \mu\text{M}$ diOMe-TPA-CN/HV system could be increased further to 14.4 due to the higher absorbance of EC characteristic peaks. Besides, the fluorescence switching responses of these two concentration systems (Fig. 11) demonstrated that EFC devices with more HV exhibited a shorter switching response time. For the 0.75/1.5 μM diOMe-TPA-CN/HV system, the excess 0.75 μM HV could increase the charge balance during oxidation. Hence, the coloring time was reduced from 11 to 3 s while the bleaching time decreased from 21 to 20 s, which indicated that obtaining electrons would scarcely be influenced by an electron-storage layer. Furthermore, when the concentration of diOMe-TPA-CN was increased twofold, the PL contrast ratio was enhanced from 8.15 to 14.4, with a switching time of 5/19 s (coloring time/bleaching time). Although the coloring time of 5 s was longer than the 3 s of the 0.75/1.5 μM diOMe-TPA-CN/HV system, it was much shorter than the 11 s of the 0.75/0.75 μM diOMe-TPA-CN/HV system, which had a 6 s shorter response time. Consequently, by just increasing the

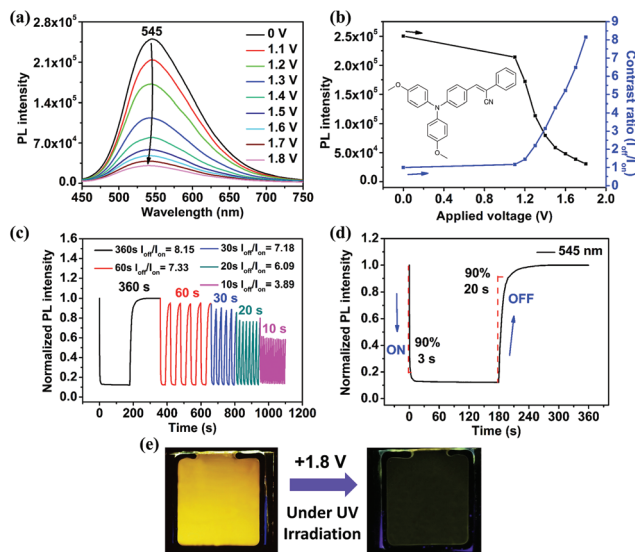


Fig. 10 (a) PL spectra at an applied voltage between 0 V and 1.8 V. (b) Applied voltage vs. PL intensity and contrast diagram. (c) Fluorescence switching response at different step-cycle times of 360, 60, 30, 20, and 10 s. (d) Estimation of the fluorescence switching time of a 0.75 $\mu\text{M}/1.5 \mu\text{M}$ diOMe-TPA-CN/HV gel-type device between 1.8 (on) and -0.1 V (off) monitored at 545 nm ($\lambda_{\text{ex}} = 408$ nm). (e) EFC behavior of a gel-type device of 0.75 $\mu\text{M}/1.5 \mu\text{M}$ diOMe-TPA-CN/HV.

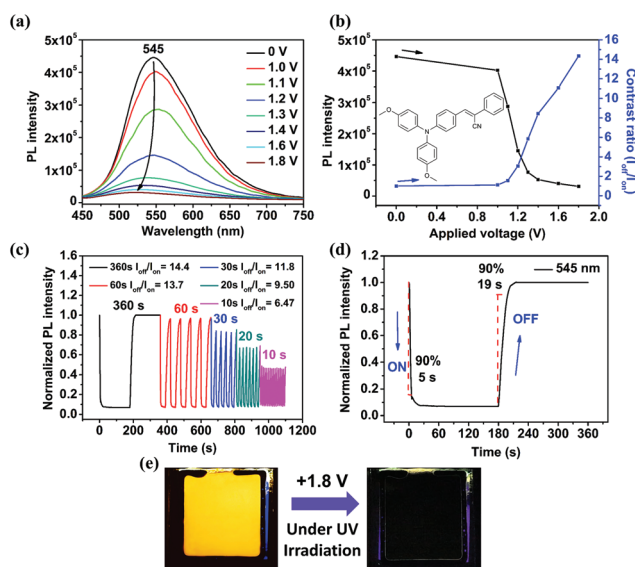


Fig. 11 (a) PL spectra at an applied voltage between 0 V and 1.8 V. (b) Applied voltage vs. PL intensity and contrast diagram. (c) Fluorescence switching response at different step-cycle times of 360, 60, 30, 20, and 10 s. (d) Estimation of the fluorescence switching time of an 1.5 $\mu\text{M}/1.5 \mu\text{M}$ diOMe-TPA-CN/HV gel-type device between 1.8 (on) and -0.1 V (off) monitored at 545 nm ($\lambda_{\text{ex}} = 408$ nm). (e) EFC behavior of a gel-type device of 1.5 $\mu\text{M}/1.5 \mu\text{M}$ diOMe-TPA-CN/HV.

concentration of HV or that of both EC materials, the resulting EFC devices shortened the switching times and increased the PL contrast ratio.

Conclusions

Novel EFC devices were fabricated by combining AIE-active molecules with a gel-type system to achieve stronger emission in the neutral state. For the purpose of reducing switching response times and increasing the PL contrast ratios of EFC devices, HV was introduced into **diOMe-TPA-CN** and **diOMe-TPA-CNBr** systems to lower working potentials, shorter switching response times, and higher PL $I_{\text{off}}/I_{\text{on}}$ contrast ratios. Furthermore, the PL contrast ratio of the EFC devices was enhanced further by tuning the ratio of the EFC material and HV in the **diOMe-TPA-CN/HV** system to acquire not only a higher PL contrast ratio of 14.4, but also a shorter EFC switching response time of 5/19 s (coloring time/bleaching time). These results demonstrate that the facile approach of combining AIE-active molecules with a gel-type system could be used to prepare novel EFC devices with stronger emission intensity in the neutral state and enhanced EFC behavior.

Conflicts of interest

There are no conflicts to declare.

Acknowledgements

This work was supported financially by the “Advanced Research Center for Green Materials Science and Technology” from the Featured Area Research Center Program within the framework of the Higher Education Sprout Project by the Ministry of Education (107L9006) and the Ministry of Science and Technology in Taiwan (MOST 107-3017-F-002-001 and 107-2113-M-002-002-MY3).

References

- J. Ye, Z. Chen, M. K. Fung, C. Zheng, X. Ou, X. Zhang, Y. Yuan and C. S. Lee, *Chem. Mater.*, 2013, **25**, 2630.
- F. Cicoira and C. Santato, *Adv. Funct. Mater.*, 2007, **17**, 3421.
- L. Y. Niu, Y. S. Guan, Y. Z. Chen, L. Z. Wu, C. H. Tung and Q. Z. Yang, *Chem. Commun.*, 2013, **49**, 1294.
- J. Luo, Z. Xie, J. W. Y. Lam, L. Cheng, H. Chen, C. Qiu, H. S. Kwok, X. Zhan, Y. Liu, D. Zhu and B. Z. Tang, *Chem. Commun.*, 2001, 1740.
- Y. Hong, J. W. Y. Lam and B. Z. Tang, *Chem. Commun.*, 2009, 4332.
- V. Goulle, A. Harriman and J. M. Lehn, *J. Chem. Soc., Chem. Commun.*, 1993, 1034.
- S. Seo, Y. Kim, Q. Zhou, G. Clavier, P. Audebert and E. Kim, *Adv. Funct. Mater.*, 2012, **22**, 3556.
- F. Miomandre, R. B. Pansu, J. F. Audibert, A. Guerlin and C. R. Mayer, *Electrochem. Commun.*, 2012, **20**, 83.
- C. P. Kuo, C. N. Chuang, C. L. Chang, M. k. Leung, H. Y. Lian and K. C. W. Wu, *J. Mater. Chem. C*, 2013, **1**, 2121.
- Y. Kim, E. Kim, G. Clavier and P. Audebert, *Chem. Commun.*, 2006, 3612.
- Y. Kim, J. Do, E. Kim, G. Clavier, L. Galmiche and P. Audebert, *J. Electroanal. Chem.*, 2009, **632**, 201.
- H. J. Yen and G. S. Liou, *Chem. Commun.*, 2013, **49**, 9797.
- J. H. Wu and G. S. Liou, *Adv. Funct. Mater.*, 2014, **24**, 6422.
- S. W. Cheng, T. Han, T. Y. Huang, B. Z. Tang and G. S. Liou, *Polym. Chem.*, 2018, **9**, 4364.
- W. Z. Yuan, P. Lu, S. Chen, J. W. Y. Lam, Z. Wang, Y. Liu, H. S. Kwok, Y. Ma and B. Z. Tang, *Adv. Mater.*, 2010, **22**, 2159.
- Y. Hong, J. W. Y. Lam and B. Z. Tang, *Chem. Soc. Rev.*, 2011, **40**, 5361.
- Q. Zhao, S. Zhang, Y. Liu, J. Mei, S. Chen, P. Lu, A. Qin, Y. Ma, J. Z. Sun and B. Z. Tang, *J. Mater. Chem.*, 2012, **22**, 7387.
- X. Y. Shen, Y. J. Wang, H. Zhang, A. Qin, J. Z. Sun and B. Z. Tang, *Chem. Commun.*, 2014, **50**, 8747.
- B. K. An, S. K. Kwon, S. D. Jung and S. Y. Park, *J. Am. Chem. Soc.*, 2002, **124**, 14410.
- Y. Xiao, L. Chu, Y. Sanakis and P. Liu, *J. Am. Chem. Soc.*, 2009, **131**, 9931.
- S. Zeng, L. Yin, X. Jiang, Y. Li and K. Li, *Dyes Pigm.*, 2012, **95**, 229.
- Y. Li, H. Zhou, W. Chen, G. Sun, L. Sun and J. Su, *Tetrahedron*, 2016, **72**, 5620.
- M. J. Percino, M. Cerón, M. E. Castro, G. Soriano-Moro, V. M. Chapela and F. J. Meléndez, *Chem. Pap.*, 2014, **68**, 668.
- A. X. Ding, H. J. Hao, Y. G. Gao, Y. D. Shi, Q. Tang and Z. L. Lu, *J. Mater. Chem. C*, 2016, **4**, 5379.
- H. J. Yen and G. S. Liou, *Polym. Chem.*, 2018, **9**, 3001.
- H. J. Yen and G. S. Liou, *Prog. Polym. Sci.*, 2019, **89**, 250.
- E. T. Seo, R. F. Nelson, J. M. Fritsch, L. S. Marcoux, D. W. Leedy and R. N. Adams, *J. Am. Chem. Soc.*, 1966, **88**, 3498.
- C. W. Chang and G. S. Liou, *J. Mater. Chem.*, 2008, **18**, 5638.
- H. S. Liu, B. C. Pan, D. C. Huang, Y. R. Kung, C. M. Leu and G. S. Liou, *NPG Asia Mater.*, 2017, **9**, e388.
- J. T. Wu and G. S. Liou, *Chem. Commun.*, 2018, **54**, 2619.